

LOW-POWER MICRO-SCALE CMOS-COMPATIBLE SILICON SENSOR ON A SUSPENDED MEMBRANE

A.Y. Kovalgin, J. Holleman, G. Iordache, T. Jenneboer, F. Falke,
V. Zieren^{*)}, and M. Goossens^{*)}

MESA⁺ Research Institute, University of Twente,
P.O. Box 217, 7500 AE Enschede, The Netherlands

^{*)} Philips Research, Prof. Holstlaan 4,
5656 AA Eindhoven, The Netherlands

In this paper we describe a new, simple and cheap silicon device operating at high temperature at a *very low power of a few mW*. The essential part of the device is a nano-size conductive link 10-100 nm in size (the so-called *antifuse*) formed in between two poly-silicon electrodes separated by a thin SiO₂ layer. The device can be utilized in chemical sensors or chemical micro-reactors requiring high temperature and very low power consumption e.g. in portable, battery operated systems. As a direct application, we mention a gas sensor (i.e. Pellistor) for hydrocarbons (butane, methane, propane, etc.) based on temperature changes due to the catalytic combustion of hydrocarbons. The power consumed by our device is at about *2% of the power* consumed by conventional Pellistors.

INTRODUCTION

“Of all the Micro Electro-Mechanical Systems (MEMS) devices being developed, chemical sensors are probably the most difficult but also the most needed (Wise, 1996)” [1].

Of a particular interest are the chemical sensors with “micro hot-plates” based on electrical conductivity changes. In such sensors, the change in the resistance of a thin conducting layer with adsorption or desorption of specific gases is monitored. These sensors pose a particular challenge: they require elevated temperatures to operate in the range between 200 °C and 600 °C. Taking into account also the overall requirement of low-power operation, using the MEMS technology for fabrication of heating/sensing device on a micro-sized suspended membrane seems to be the most appropriate approach.

As an important application example of micro hot-plate chemical sensors, a gas sensor for hydrocarbons (butane, methane, propane, etc.) can be considered, i.e. the so-called Pellistor [2]. Such a sensor is based on temperature changes due to the catalytic combustion of hydrocarbons. A mixture of a combustible gas with oxygen diffuses into the porous catalyst-containing material, which covers the hot plate, and reacts there with the catalyst. This leads to the local burning of the mixture and gives an extra amount of heat resulting in a higher local temperature. This temperature increase can be monitored

by the change of the electrical resistance of the device. The use of a Pellistor is therefore based on a) the ability of a heating element to maintain a required temperature inside the porous coating layer with a catalyst, and b) the ability to sense an extra heat developed due to the catalytic combustion in that layer.

One significant drawback of a conventional Pellistor is its relatively high power consumption. The commercial sensing devices use a platinum wire as a heating/sensing element and require a power of about 100 mW. Other types of pellistor-like devices realized more recently on suspended membranes employ a meander-like pattern of a conductive layer as platinum or poly-silicon and still require about 20-40 mW [3]. To realize an electrical resistance of a few kOhms, the dimensions of the meander and the corresponding suspended membrane have to be relatively large, in the order of hundreds of microns. These devices once fabricated have a certain resistance, which can not further be changed.

Our work employs the idea of maintaining a micro-sized hot surface-area by means of dissipating power at a nano-scale conductive link created between two micro-scale poly-silicon electrodes separated by a dielectric [4]. In comparison to a conventional Pellistor, the link is only 10-100 nm in size and requires a power of 1-3 mW to keep a suspended plate of several microns in diameter at high temperatures up to 600 °C. Furthermore, the link resistance can finely be tuned in the range between a few kOhm and 100-200 Ohm by electrical programming at the appropriate current [4-6]. This allows for tuning the consumed electrical power for each device individually. In contrast to the conventional Pellistors, adjusting the electrical resistance for our device by an appropriate electrical programming can be considered as an advantage.

In this paper, we describe a silicon sensor (the so-called *antifuse*) resembling a very low power Pellistor for hydrocarbons. The power consumed by our device is at about 2% of the power consumed by conventional Pellistors. To meet the low power requirements, two main challenges were addressed: a low power heater and good thermal isolation from the substrate. The best option was to use a micro-hotplate and a nano-scale antifuse as a heating/sensing element built on a suspended membrane.

In general, the MEMS technology does not match with the CMOS technology due to the restrictions posed by the device fabrication. For example, serious limitations are implied if the “release etch” is performed after aluminum contact pads are already realized on the wafer. In this paper, we demonstrate a simple, low cost procedure, which allows for the membrane release to be performed as a last processing step after the fabrication of the antifuse device is completed, with the aluminum bonding pads exposed. For poly-Si sacrificial layer and silicon bulk, a selective etchant was used, not attacking the masking oxide, nitride membrane or the aluminum patterns.

DESIGN

To enable a highly sensitive Pellistor-type gas sensor, the power density per unit surface area required to maintain this hot area has to be very low. Therefore, good thermal isolation is considered to be an important issue. To minimize the heat losses by

thermal conductivity, the antifuse-based heater has been realized on a suspended membrane.

The essential part of our device is a nano-scale conductive link of 10-100 nm in size (the so-called *antifuse*) formed in between two poly-silicon electrodes separated by a thin SiO₂ layer (Fig 1). To create a silicon-SiO₂-silicon antifuse, the insulating SiO₂ layer between the electrodes is destroyed (*antifused*: insulator becomes conductive) by a two-step electrical stress, during which the insulator melts locally [4, 6]. The link formed has a resistor-like behaviour, so if a current is passing through the antifuse, it can generate heat. The link also acts as a heat detector (i.e. thermo resistor) because its resistance is a sensitive measure of its temperature.

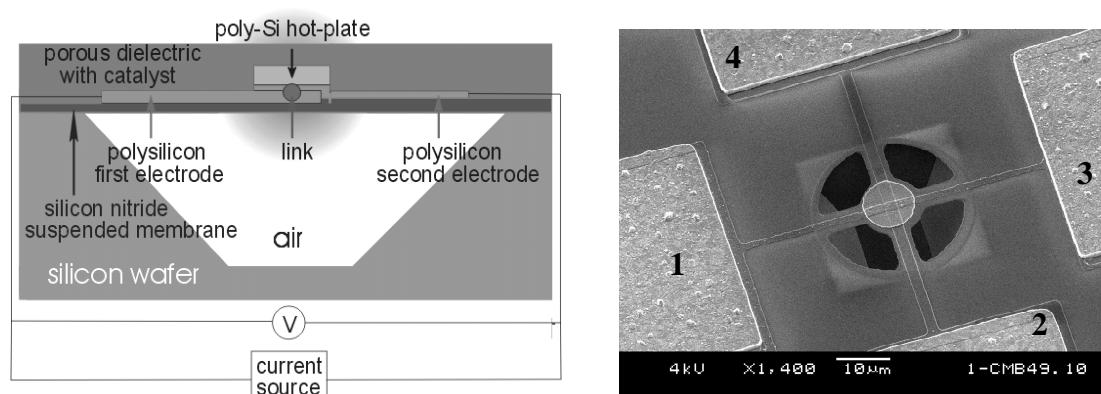


Figure 1: Schematic drawing of the nano-hot-spot antifuse device on a nitride suspended membrane (left) and SEM image of a realized device (right).

In the structure shown on the right-hand side in Fig 1, poly-silicon lines 1→3 and 2→4, crossing each other in the centre, correspond to the two abovementioned poly-silicon electrodes. A 10-nm thick silicon dioxide layer is deposited in between the electrodes to separate them and avoid an electric contact. The resistance of each poly-line between the square aluminum pads (i.e. lines 1→3 and 2→4) is measured in the range of 1-4 kOhm. Before electrical programming, i.e. before a conductive link between contacts 1 and 2 is established, there is a very low leakage current flowing from 1 to 2. During the programming, the link is controllably enlarged by means of applying a current stress. After the programming, a conductive link-antifuse is finally created between the poly-lines. The resistance between the poly-lines, i.e. the antifuse resistance, can be varied in the range of 2 kOhm - 100 Ohm, depending on the programming current.

A 200-nm thick poly-Si disk of 10 μm in diameter (the actual hot plate placed above the second poly-line) is designed to uniform the surface temperature. Additionally, a 300-nm thick porous aluminium oxide layer doped with a catalyst is applied to the surface.

During a standard operating mode, a current is forced between contacts 1 and 2 and the voltages across 1 and 2 and across 3 and 4 are measured. This allows for measuring the total electrical resistance of the structure R_{tot} , i.e. the resistance of the antifuse link in series with the resistance of the poly-silicon electrodes, and at the same time the resistance of the link R_{link} only. The method offers the advantage that driving and measuring of the device are decoupled.

An extra advantage of the proposed concept is *decoupling the electrical resistance and thermal resistance*. In conventional hot plate devices, the heat is obtained either from the filament heater or suspended poly-silicon meander. In such a design, an increase of thermal resistance of the electrical leads is an important issue due to the necessity to minimize the power loss through the leads. Indeed, an increase of the thermal resistance can only be achieved by shrinking the cross-sections, which gives rise to the increasing electrical resistance resulting in undesired extra power dissipation. In this paper, a new concept is proposed with independent control of both the resistances. Decoupling becomes possible because the electrical resistance is now determined by the link resistance only and has no influence on the thermal resistance due to the nano-scale link dimensions. In other words, the devices are designed in such a way that one can manipulate the heat flow in the bulk of the device without affecting its electrical resistance.

NUMERICAL MODELLING

To verify the ability of the nano-hot-spot antifuse device to maintain a high surface temperature at a power consumption of a few mW, we have carried out numerical simulations using SILVACO code [7]. As one can see in Fig 2, the power consumption can strongly be influenced by the link diameter. The smaller the link, the higher the resistance of the link. In other words, the role of the link in the entire heat generation process increases if link dimensions become smaller. For a smaller link, less heat can be generated in the poly-silicon lines meaning that the power losses in the lines will also decrease. The latter is a direct result of the abovementioned concept of decoupling the electrical and thermal resistances of the device.

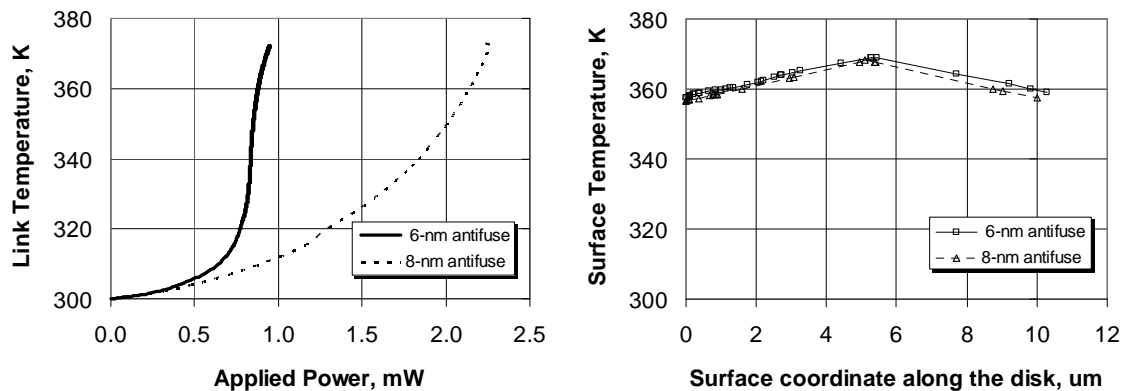


Figure 2: Left – modelled maximum device temperature versus applied power for the nano-hot-spot antifuse device shown in Fig. 1; Right – modelled horizontal temperature distributions in the aluminum oxide layer deposited on the 10-um poly-Si disk.

It appears from our modelling that a link of 6 nm in diameter can heat the surface up to 100 °C by absorbing electrical power of 0.9 mW only (Fig 1, left). A bigger link of 8 nm in diameter requires about 2.3 mW to maintain the same surface temperature distribution. Unfortunately, with increasing the temperature beyond 100 °C some problems related to the convergence of the solutions have occurred in the simulator.

However, from Fig 2 it can clearly be seen that, in case of the smallest link, the surface temperature increases very rapidly with the power. Extrapolating, for a link of 6 nm in diameter one can expect a temperature of 600 °C for a power of 1.5-2 mW. For smaller links, the power consumption is expected to be even lower.

From the results of modelling we can conclude that, for our nano-hot-spot antifuse device on a suspended membrane, maintaining a surface temperature in the range of 200-600 °C looks feasible at a dissipated electrical power not exceeding a few mW.

DEVICE REALIZATION

We developed a *fully clean room CMOS compatible*, simple and low cost method for processing of thermally isolated suspended membranes. The method allows for the “release” etch of the membranes with devices already fabricated and aluminum bonding pads patterned. For the “release” etch, a selective etchant was used, not attacking the masking oxide, nitride membrane, and the aluminum patterns [8]. Such an anisotropic wet etchant enables “self-stopping” at the (111) crystallographic planes of the Si substrate.

To minimize the heat losses by thermal conductivity, a very low-power antifuse heater has to be fabricated on a suspended membrane. There is a trade-off in choices between mechanical and thermal properties of the potential materials to be used for the suspended membrane. Silicon nitride has a higher thermal conductivity coefficient than silicon oxide, but better mechanical properties so that we designed the structure on a 100-nm thick stress-free silicon nitride. As a result, the only main contribution to the thermal conductivity losses is from the 2-microns wide, 100-nm thick poly-silicon electrodes of the antifuse, and the 4-microns wide beams of the suspended membrane as in Fig 1 above.

We start the processing with growing a 500-nm thick oxide layer on a standard (100) Si wafer (Fig 3a). The oxide is patterned and windows are etched in BHF in the places where the suspended membranes are to be fabricated (Fig 3b). Next, a 550-600-nm thick poly-silicon layer is deposited to cover the wafer (Fig 3c). Further, Chemical Mechanical Polishing (CMP) is employed, to remove the excess poly-silicon and some of the oxide down to a 400-450-nm thick layer (Fig 3d). This thickness is not critical for our design and was chosen to make sure there is no poly-silicon left on top of the oxide. The poly-silicon in the trenches is the layer to be used as a sacrificial layer at a later stage when releasing the suspended membrane. After the CMP, the surface of wafer is even and smooth. As the next step, the membrane-to-be 100-nm stress-free silicon nitride layer is deposited on the polished surface and further on, the antifuse devices are fabricated (Fig 3e). This comprises deposition and patterning of a two highly doped 100-nm thick poly-silicon layers (i.e. electrodes), a 10-nm thick LPCVD oxide in between, and a poly-Si disk of 10 μ m in diameter on top. The disk acts as a micro-hot-plate and can be observed in the SEM micrograph in Fig 1. For simplicity, the poly-silicon micro-hot-plate is not included in the drawings in the Fig 3. After fabrication, the antifuse structures are passivated by a 20-nm thick SiO₂ deposited by LPCVD and aluminum bonding pads are

realized. Next, plasma etching is performed to open windows into the nitride layer (Fig 3f).

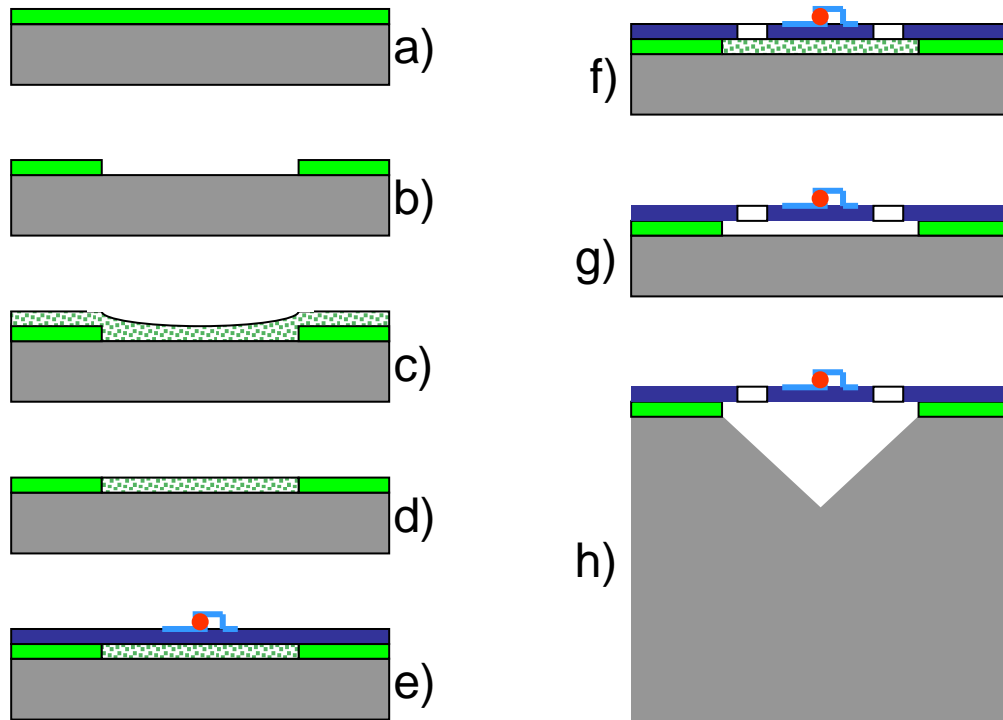


Figure 3: Processing steps for the nano-hot-spot antifuse device on a thermally isolated suspended membrane.

Finally, the “release” etch is done by wet etching the sacrificial poly-silicon layer underneath the nitride membrane (Fig 3g). Etching is carried on with the bulk silicon substrate to realize an inverted pyramid cavity, for even better thermal insulation (Fig 3h). We have used a selective etchant that does not etch aluminum [8, 9]: 5 wt. % TMAH solution, 1.6 wt. % dissolved silicon and 0.5 wt. % $(\text{NH}_4)_2\text{S}_2\text{O}_8$. TMAH stands for tetra methyl ammonium hydroxide and $(\text{NH}_4)_2\text{S}_2\text{O}_8$ is ammonium peroxy-disulfate that plays a role of an oxidant additive here. The use of a traditional 1% KOH etchant is not possible due to a) the aluminum bonding pads are already fabricated on the wafer, and b) KOH is not a clean room CMOS compatible chemical [10]. Furthermore, the etching method in TMAH is faster as about 16- μm deep inverted pyramid cavities are etched in the substrate during 30 min.

An important problem in MEMS technology is the way to deal with the specific packaging challenges. A MEMS processed wafer cannot be diced with exposed devices. Our approach offers the advantage that wafer bonding is avoided and even more, the release etch could be performed after the complete fabrication of any other required devices on the membrane, after metallization and even after dicing of wafer, on a chip level.

EXPERIMENTAL RESULTS AND DISCUSSIONS

Electrical Characterization and Link Temperature Estimation

The conductive link between the two electrodes (i.e. *an antifuse*) is initially caused by electrical breakdown due to tunnelling a constant current stress through the 10-nm thick gate oxide. Finally, we apply a well-defined programming current, which is higher than the initial stressing current, to enlarge the link [4]. It appears from our research that as the link is once created at certain value of the programming current, the size and electrical properties of the link cannot be changed under a current stress below the programming value. Both the programming and electrical characterisation have been carried out using a parameter analyser Agilent 4156C.

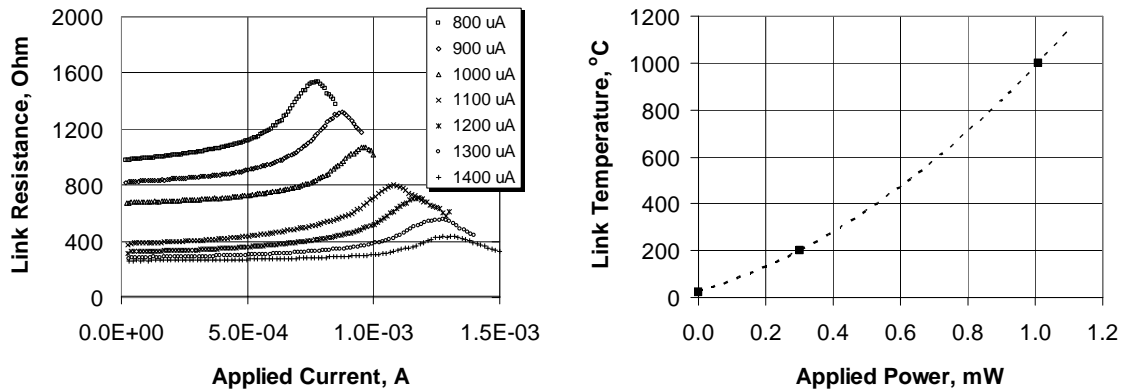


Figure 4: Left – dependence of the link (antifuse) resistance on applied current at different stages of programming the device; Right – estimated link temperature versus power for another device with a link resistance of about 1 k Ohm at room temperature.

Measuring the resistance versus current passing through the link, one can clearly observe a resistance increase above certain currents (Fig 4, left). This can be attributed to the metallic behaviour of the poly-silicon and therefore indicates a temperature rise of the antifuse. A maximum resistance can be obtained at different currents, depending on the previously applied current. The maximum corresponds to the intrinsic point of silicon and can be estimated at about 1000 °C for the doping concentration used. Starting from this point, the heat-generated carrier concentration exceeds the doping concentration, which leads to the resistance drop. Further increase of current/power causes re-melting the link (1415 °C for Si) and results in its bigger diameter and, therefore, lower resistance. This step is called re-programming and can additionally be affected by an irreversible change in the link material quality due to the high temperature. For example, a diffusion of the impurity atoms can take place. As the temperature required for sensing combustible gases when using a catalyst is much lower, standard operating conditions disable re-programming.

The extrapolation done using the results presented in Fig 2 show that a link of 6 nm in diameter is expected to maintain a surface temperature about 600 °C by absorbing 1.5-

2 mW of electric power. As appears from the same simulations, the antifuse link itself, situated in the core of the device, has similar temperature. This temperature is not significantly higher than the surface temperature due to the high thermal conductivity of poly-silicon used as a hot plate. So the heat can properly be transferred from the link to the surface without essential losses. To estimate the core temperature (Fig 4, right), the resistance of the antifuse was plotted against the current with the chuck temperature at 25 °C and 200 °C respectively. If we accept that the resistance of the antifuse is only a function of the temperature then equal resistance should mean equal temperatures. At certain current the “25 °C” resistance reaches the same value as the “200 °C” resistance at near zero current. This can be considered as the first calibration point of the “25 °C” curve. A second calibration point is where the derivative of the resistance becomes zero. This is the intrinsic point of the heavily doped silicon. For a doping level of 10^{20} atoms/cm³, the intrinsic point is approximately at 1000 °C. So this can be considered as a second calibration point. The third calibration point corresponds to 25 °C at zero current. The right-hand graph in Fig 4 shows the results of such a temperature calibration for a link with a resistance of about 1 kOhm at room temperature.

Stability Tests

A number of stability tests have been carried out. A typical device shown in Fig 5 was kept at 70% of the link programming power for 15 hours. The link was programmed at 0.58 mW meaning the power dissipated in the link only. The intrinsic point attributed to 1000 °C was observed at a power of 0.55 mW. Applying the same procedure as we used for plotting the right-hand graph in Fig 4, we can estimate the link temperature in the range of 600-800 °C. This is caused by dissipating 70% of the programming power (i.e. 0.4 mW). We noticed instabilities ($\pm 10\%$) during the first 3 hours of operation and rather reasonable stability within 1-2% for the rest of the time.

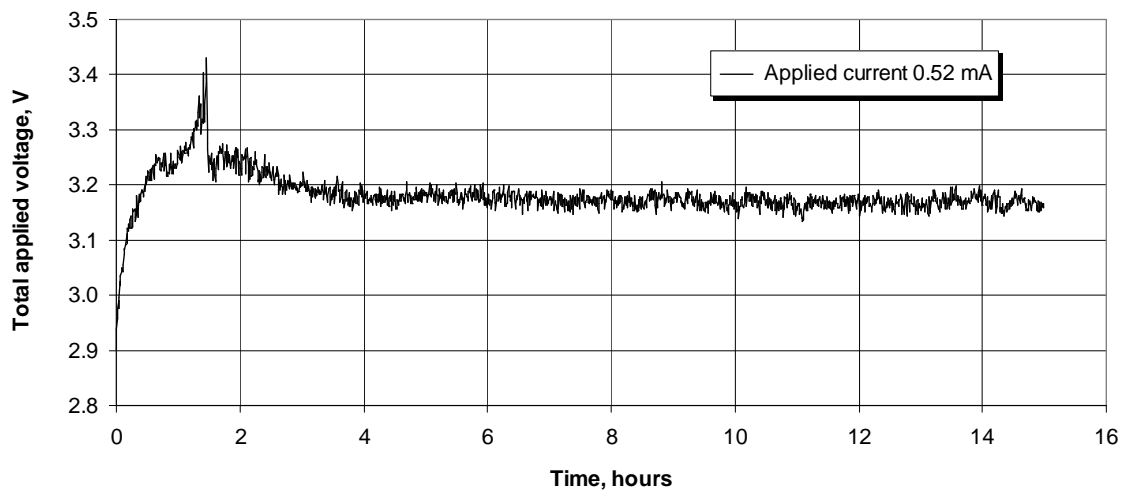


Figure 5: Result of a stability test for 15 hours; the device was kept at 70% of the link programming power, which corresponds to the temperature of 600-800 °C.

Surface Temperature Mapping

The surface temperature mapping has been carried out using IR thermal radiation measurements by slow-scan CCD camera. Images were captured on a Leitz microscope with a 125x/NA=0.8 objective lens. The camera used was a Princeton Instruments TE-512, back-illuminated, VIS-AR coated CCD. Background signal was captured with device current off. This signal was subtracted for each pixel from the “current-on” images taken in the same exposure time interval.

A separate calculation has been done to determine the sensitivity of this camera to thermal radiation, involving Planck’s Law and the camera’s quantum efficiency. The signal was expressed in counts/s for a given surface (blackbody) temperature and emissivity ϵ . The latter is not known, but we expect the value of ϵ to be between 0.4 and 0.9 (when Si is coated by Al_2O_3). Some references give $\epsilon_{\text{Si}}(T)$ between 0.4 and 0.6 for a wavelength λ between 400 nm and 1000 nm and temperature from 300 to 800 °C ($\epsilon_{\text{Si}} = 0.68$ at room temperature and 1 μm wavelength). The calibration curve for a fixed value of ϵ has not yet been fully verified experimentally, i.e. the shape was verified, but the transmission factor of the total optical system was not yet included, and set to 1 for the moment.

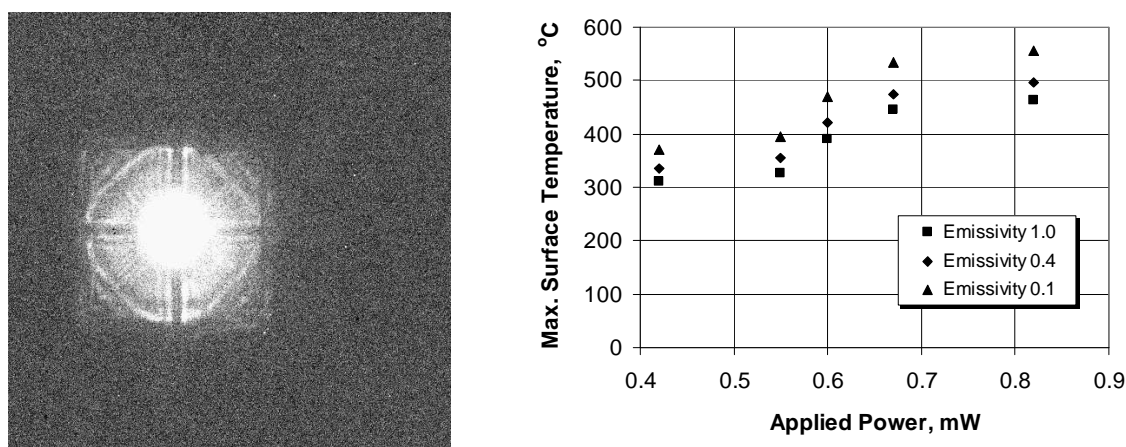


Figure 6: Left – CCD image; Right – surface temperature, calculated on the basis of the CCD image, versus applied power.

From the measurements, maximum temperature seems not to exceed 600°C at dissipated power of 0.8 mW (Fig 6). This is in good agreement with our previous considerations. In the thermal image, one can clearly recognize the bright disk in the centre corresponding to the hot plate, and the poly-silicon lines. The surface temperature is uniform within 30-40 °C for the bright disk. This is in good agreement with the uniformity of 10-15 °C obtained from the simulations (Fig 2).

Experiments on Gas Sensing

To confirm the feasibility of the devices to maintain a hot surface and perform as Pellistor-type sensors, we carried out a number of gas sensing experiments. It has to be

emphasized that the devices are not only intended to maintain certain temperature on the surface but also to monitor the temperature change, which is a measure of the surface process. In Fig 7 (left) one can notice a clear response after butane is introduced into the measuring chamber. From the fact that the response peaks are directed upwards, we can further conclude that the resistance of the device increase after the gas is introduced. This change of the resistance can be attributed to a temperature increase caused by an exothermic process (e.g. combustion) at the device surface. If such a process takes place, the produced extra heat will increase the device temperature and cause the resistance increase according to Fig 7 (left).

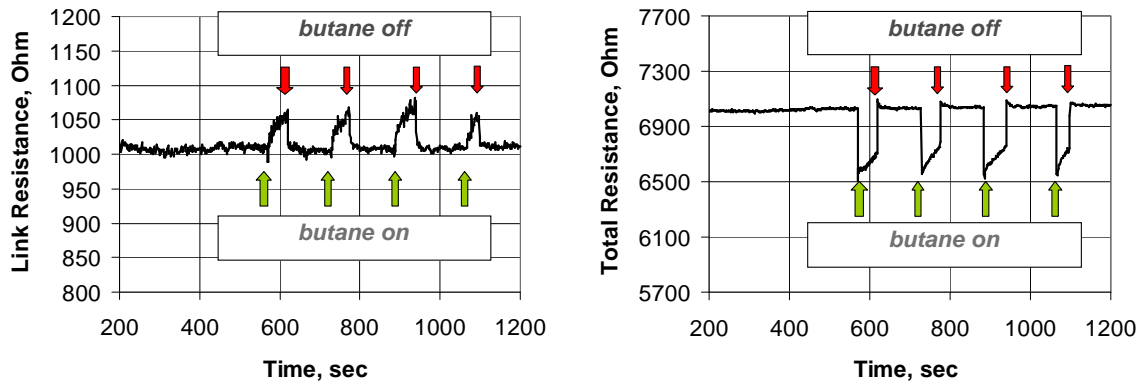


Figure 7: Gas sensing experiments.

It is interesting to note that two effects play a role at the same time. The decrease in total resistance R_{tot} (Fig 7, the right plot) may be related to a thermal conductivity effect that takes place between the membrane and its poly-Silicon patterns and the cavity walls. Since the poly electrodes are on average closer to these walls than the hot plate they are more sensitive to conductivity changes. This may counteract the increase of the resistance of the link R_{link} in the presence of butane, which is a result of the catalytic activity as explained above. By using a device with catalyst and one without catalyst in a Wheatstone bridge design the changes caused by the thermal conductivity effect can be ruled out.

CONCLUSIONS

We developed a *fully clean room CMOS compatible*, simple and low cost method for processing of thermally isolated suspended membranes. The method allowed for the “release” etch of the membranes with devices already fabricated and aluminum bonding pads patterned. For the “release” etch, a selective anisotropic wet etchant was used, which enabled “self-stopping” at the (111) crystallographic planes of the Si substrate.

The type of device we described is worth considering when chemical sensors or chemical micro-reactors requiring a high temperature and very low power consumption are to be realized, as in portable, battery operated systems. As a direct application, we have demonstrated the use of our device as a Pellistor-type gas sensor for hydrocarbons.

Both the experiments and simulations indicate that the devices are able to maintain a surface temperature as high as a few hundred degrees centigrade at power consumption in the range of a few mW. This corresponds to about 2% of the power consumed by conventional Pellistors.

ACKNOWLEDGEMENTS

This work was financially supported by the EU project SAFEGAS (GRD1-1999-10849). We are grateful to H. Kruidhof, M.W.J. Luiten, and S. Ebessen of the Department of Chemical Technology, University of Twente, for their guidance on making the porous layer with catalyst.

REFERENCES

1. "Chemical Sensing Using MEMS Devices" in "Opportunities in Biotechnology for Future Army Applications" (2001), NATIONAL ACADEMY PRESS 2101 Constitution Avenue, N.W. Washington, DC 20418; ISBN: 0-309-50303-5, pp.92-95. Available online at:
<http://books.nap.edu/books/0309075556/html/92.html#pagetop>
2. M. Gall. *Sensors and Actuators B (Chemical)* **B4**, 533-8 (1991).
3. Cs. Dücső, M. Ádám, P. Fürjes, M. Hirschfelder, s. Kulinui, and I. Bársony. Eurosenors 2002 – Book of Abstracts, edited by J. Saneistr and P. Ripka, ISBN 80-01-02576-4, pp. 525-526.
4. V. E. Houtsma, Ph.D. Dissertation, University of Twente, Enschede, The Netherlands, ISBN 90-365-1391-X (1999).
5. A. Y. Kovalgin, J. Holleman, A. van den Berg. In "*Sensor Technology 2001*", Proceedings of the Sensor Technology Conference 2001, Enschede, the Netherlands. Ed. M. Elwenspoek, Kluwer Academic Publishers, p. 107-112, ISBN 0792370120, (2001).
6. A.Y. Kovalgin, J. Holleman, A. van den Berg. Eurosenors 2002 – Book of Abstracts, edited by J. Saneistr and P. Ripka, ISBN 80-01-02576-4, pp. 31-32.
7. SILVACO International: Athena user's manual and Atlas user's manual (device simulation software), April 1997.
8. G.Yan, P.C.H.Chan, I-Ming Hsing, et.al., *Sensors and Actuators A* **89** (2001), p. 135-141.
9. J.T.L. Thong, W.K. Choi and C.W. Chong, *Sens. Actuators A* **63** (1997), pp. 243–249.